



Dynamic Meteorology-Induced Emissions Coupler (MetEmis) development in the Community Multiscale Air Quality (CMAQ): CMAQ-MetEmis

5 Bok H. Baek¹, Carlie Coats¹, Siqi Ma^{1,2}, Chi-Tsan Wang¹, Jia Xing¹, Daniel Tong^{1,2}, Soontae Kim⁴, and Jung-Hun Woo^{3*}

¹Center for Spatial Information Science and Systems, George Mason University, Fairfax, VA 22030, USA

²Department of Atmospheric, Oceanic and Earth Sciences, George Mason University, Fairfax, VA 22030, USA

³Civil and Environmental Engineering, College of Engineering, Konkuk University, Seoul, Republic of Korea

⁴Environmental Engineering, College of Engineering, Ajou University, Suwon, Republic of Korea

10 *Correspondence to:* Jung-Hun Woo (jwoo@konkuk.ac.kr)

Abstract

The main focus of this study is to develop a dynamic-coupling “inline” air quality modeling system for the meteorology-induced emissions with simulated meteorological data. To improve the spatiotemporal representations and accuracy of onroad vehicle emissions, which are largely sensitive to local meteorology, we developed the “inline” coupler module called “MetEmis” for Meteorology-Induced Emission sources within the Community Multiscale Air Quality (CMAQ) version 5.3.2 modeling system. It can dynamically estimate meteorology-induced hourly gridded emissions within the CMAQ modeling system using modeled meteorology. The CMAQ air quality modeling system is applied over the continental U.S. for two months (January and July 2019) for two emissions scenarios: a) current “offline” based onroad vehicle emissions, and b) “inline” CMAQ-MetEmis onroad vehicle emissions. Overall, the “MetEmis” coupler allows us to dynamically simulate onroad vehicle emissions from the MOVES onroad emission model for CMAQ with a better spatio-temporal representation compared to the “offline” scenario based on static temporal profiles. With an instance interpolation calculation approach, the new “inline” approach significantly enhances the computational efficiency and accuracy of estimating mobile source emissions, compared to the existing “offline” approach that yields almost identical hourly emission estimation. The domain total of daily VOC emissions from the “inline” scenario shows the largest impacts from the local meteorology, which is approximately 10% lower than the ones from the “offline” scenario. Especially, the major difference of VOC estimates was shown over the California region. These local meteorology impacts on onroad vehicle emissions via CMAQ-MetEmis revealed an improvement in hourly NO₂, daily maximum ozone, and daily average PM_{2.5} patterns with a higher agreement and correlation with daily ground observations.

Keywords: CMAQ, CTM, weather-aware emissions, vehicle emissions, inline modeling

1. Introduction

35 Since the industrial revolution, the chemical pollutants in the atmosphere have impacted human society due to their adverse health effects. The primary gases and particles directly emitted from their emission sources are chemically transformed into secondary pollutants through complex chemical reactions under various local meteorological conditions. Over last three decades, sophisticated multiscale chemical transport models (CTM) have been developed to predict the concentrations of primary and secondary chemicals in the lower



40 atmosphere, and actively used for air quality regulatory planning applications as well as for air quality
forecasting for the general public health (Wong et al., 2012; Byun and Schere, 2006; Dennis et al., 2010; Rao
et al., 2011; Hogrefe et al., 2001). The CTM simulation results strongly rely on two major inputs:
meteorology and emissions, thus requiring accurate estimation of both to simulate the transport, chemical
45 transformation, and removal of the pollutants. Depending on their chemical reactivity and gravitational
behaviors, some pollutants can be chemically transformed and travel a long distance from their source of
origin while some are deposited near their release locations.

To accurately predict regional and global chemicals in the future, spatially and temporally resolved
meteorology and emissions are critical and required to be rapidly updated based on the aerosol direct/indirect
meteorology impacts within a fully coupled air quality modeling system. There have been considerable
50 amounts of efforts in meteorology prediction enhancements actively conducted (Jacob and Winner, 2009;
Grell and Baklanov, 2011; Fiore et al., 2012; Wong et al., 2012). However, there have been only limited
“*inline*” emissions modeling enhancements made to CTM system wherein emissions from meteorologically
driven air pollutant emission processes are dynamically coupled within the regional/global CTM modeling
system, rather than being estimated *a priori* and statically provided as model inputs based on “offline” spatial
55 and temporal allocations. Simulating emissions “*inline*” is especially crucial for real-time air quality
forecasting (Tong et al., 2012). In particular, the system of the National Oceanic and Atmospheric
Administration (NOAA) National Air Quality Forecast Capability (NAQFC) allows to induce the influences
of the forecast meteorology on emissions from key sources, such as stationary power plants, vegetation,
fertilizer applications, such as mineral dust (Knippertz and Todd, 2012), sea salt (Foltescu et al., 2005; Pierce
60 and Adams, 2006), biogenic volatile organic compounds (BVOCs) (Lathière et al., 2005; Chen et al., 2018),
and biomass burning events (Grell et al., 2011; Pavlovic et al., 2016). Despite these scientific advancements
and model improvements, true process-based interaction between local meteorology and meteorology-
induced anthropogenic pollutant emissions from onroad vehicles, livestock wastes, and residential heating
remain incomplete or overlooked (Pouliot, 2005; Tong et al., 2012).

65 The mobile/transportation sector is one of the most important anthropogenic emissions sectors in
metropolitan regions where most of high ozone and PM_{2.5} concentration episodes often occur (Andrade et al.,
2017; Kumar et al., 2018; Perugu, 2019). It is also known that the performance and emissions of mobile
engines are sensitive to local weather conditions, such as ambient temperature and humidity (Lindhjem et al.,
2004; Iodice and Senatore, 2014; Choi et al., 2017; Mellios. et al., 2019). The incomplete fuel combustion
70 can be occurred under cold ambient temperature and high humidity, leading to higher emissions emitted. The
effect of humidity on internal combustion engines, including spark-ignition engines (gasoline, LPG, and
natural gas) and compression ignition or diesel engines, has been known for many years, with evidence
indicating that higher humidity results in lower NO_x emissions(Lindhjem et al., 2004; USEPA, 2015).
Additional emissions also come from energy usage of air conditioning at higher ambient temperatures. These
75 meteorological impacts can be accounted for using the state-of-science mobile emissions models such as the
U.S. EPA’s MOTO Vehicle Emission Simulator (MOVES) version 3.0 (USEPA, 2020). However, it lacks
transparency of air pollutant emission algorithms, including key parameters such as emission factors.
Furthermore, it requires significant computational resources to generate these high-quality spatiotemporal
emissions from onroad vehicles (Li et al., 2016; Xu et al., 2016; Liu et al., 2019; Perugu, 2019). To provide
80 the weather-aware onroad mobile emissions to the current CMAQ, the MOVES has been integrated with the
Sparse Matrix Operator Kernel Emissions (SMOKE) modeling system (Baek et al., 2010) by processing
(reading/storing/accessing) MOVES emission factors (EF) datasets. However, it demands a significant
computational time and memory due to the high traffic of input/output (I/O) data, which largely prohibits its



usage in real-time air quality forecasting. As an example, the latest version of SMOKE version 4.8.1 can
85 require >3 computing hours with up to 20GB RAM memory to generate 25 hours CMAQ-ready gridded
hourly emissions over Continental U.S. (CONUS) modeling domain (12km *12km grid size).
To enable the direct feedback effects of aerosols and local meteorology in an air quality modeling system
without any computational bottleneck, we have developed an “*inline*” meteorology-induce emissions coupler
module within the US EPA’s CMAQ modeling system, called “Meteorologically-induced anthropogenic
90 Emissions: CMAQ-MetEmis”, to dynamically model the complex MOVES onroad mobile emissions inline
without a separate dedicated emissions processing model like SMOKE. To address the shortcomings
(computational time and memory requirements) in the current slow “*offline*” approach, we first re-
restructured the current CMAQ-ready surface gridded hourly emissions output from SMOKE into the
ambient temperature-specific gridded hourly emissions and store them into a pseudo-layer structure for easy
95 and fast access. Each pseudo-layer holds the gridded chemically-speciated hourly emissions by incremental
temperature bin (e.g., 10F, 20F, and so on). The CMAQ-MetEmis coupler was developed to estimate the
gridded hourly emissions with a simple linear interpolation between two temperature-bins gridded hourly
emissions based on a simulated hourly ambient temperature. With an instance interpolation calculation
approach, the new “*inline*” approach significantly enhances the computational efficiency compared to the
100 existing “*offline*” approach without losing any accuracy of emission estimates. We also evaluate the
performance of the CMAQ-MetEmis coupler module in CMAQ which includes their computational
performance, the feasibility of CMAQ-MetEmis implementation as a forecasting application, the responses
of O₃ and PM_{2.5} to the meteorological impacts on anthropogenic emissions.

2. CMAQ-MetEmis Development

105 NOAA has developed the NAQFC, operated by the National Weather Service (NWS), in partnership with
the U.S EPA using the state-of-science air quality modeling system, CMAQ, to forecast concentrations of O₃
and PM_{2.5} over the contiguous continental U.S. (CONUS), Alaska and Hawaii (Tong et al., 2015; Lee et al.,
2017; Tang et al., 2017). Unlike weather forecasting, air quality forecasting requires full atmospheric
chemistry along with the physical state and tendency of the weather in the near future. Accurate prediction
110 of meteorology and emissions for CMAQ plays a critical role in the accuracy of 48- and 72-hour air quality
forecasting. The current NOAA/NWS operational requirements specify that the post-processing of the
simulated/forecasted meteorological data, emission data, and air quality chemistry model simulations be
completed in a reasonable time frame to meet the air quality forecasting time constraints. Since the
processing of the meteorological data and the execution of the air quality chemistry model are the most time-
115 consuming part of CMAQ, minimizing the processing time of the emissions needs is desirable. A typical
emission-processing over U.S. CONUS national domain for one day may take up to 2 hours on a single CPU
(Intel Xeon Gold 6240R @ 2.4GHz) using SMOKE and other post-processing tools. To expedite the
operational forecasting streamlines, non-meteorological dependent emissions are generally processed in
advance (Tong et al., 2015). Only the meteorologically induced emission sources are processed during the
120 air quality forecasting simulation runs. So then, the accuracy of the emission processing can be maintained,
and the forecast can be completed within the required time constraints. However, due to the high computing
CPU hour requirement to estimate the high-quality onroad mobile emissions from MOVES, the SMOKE-
MOVES integration tool that allows dynamically estimating weather-aware gridded hourly emissions with
the forecast meteorology from NAQFC has not been implemented in the current NAQFC operations (Tong
125 et al., 2015).



2.1 Modeling Configuration

The George Mason University (GMU) air quality modeling system in this study is configured close to the current operational NAQFC, including the spatial coverage, emission inputs, and chemical transport model.

130 It contains three major components: meteorology, emission, and chemical transport models. The Weather Research and Forecasting (WRF) model version 4.0 is used to generate hourly meteorological fields to drive emission and air quality modeling. The WRF model was configured with Thompson graupel microphysics scheme, RRTMG long and short-wave radiation scheme, Mellor-Yamada-Janjic PBL scheme, unified Noah land-surface model, and Tiedtke cumulus parameterization option. The emission input was provided using a
135 hybrid emission modeling system that utilized the SMOKE model version 4.8.1 (Baek and Seppanen, 2021) to process anthropogenic emissions, and a suite of emission models to estimate emissions from intermittent and/or meteorology-dependent sources. Anthropogenic emissions were taken from US EPA 2017 NEI. The CMAQ model (version 5.3.2) ingests emissions and meteorology to predict spatial and temporal variations of the atmospheric pollutants (such as O₃, NO_x, and particulate matters) using a revised Carbon Bond 6 gas-phase mechanism and AE7 aerosol mechanism (CB6r3_AE7_AQ) (Byun and Schere, 2006; Luecken et al.,
140 2019).

The meteorological, emission and air quality models have 12×12 km horizontal resolution over the contiguous United States, with full 35 sigma layers vertically and the domain top at 50 hPa. The WRF model was driven by the forecast fields of Global Forecast System (GFS) version 4 products with a horizontal
145 resolution of 0.25° × 0.25° (available every 6 h) and was reinitialized every 24 hr to be consistent with its operational task.

To understand the impacts of meteorology-induced onroad emissions on local air quality, we conducted two CMAQ simulation scenarios. All simulations were conducted for two months, January and July in the year 2019. We initiated our CMAQ simulations based on the default CMAQ background concentration profiles.

150 The first three days of CMAQ simulation were used as a spin-up modeling period to eliminate the influence of the initial condition (Chen et al., 2021; Lv et al., 2018; Tong and Mauzerall, 2006). The configurations and simulations are listed in Table 1.

1. “Base” scenario: Static gridded hourly emissions based on the county total emissions with static
155 temporal profiles (monthly, weekly, month-to-day, and hourly).
2. “MetEmis” scenario: Weather-aware gridded hourly emissions dynamically simulated with simulated meteorology using the inline “CMAQ-MetEmis” approach.

2.2 Meteorology-Depended Mobile Emissions

160 Mobile emissions from onroad and off-network (e.g., vehicle start-up, running exhaust, break-tire wear, hot soak, and extended idling) are much sensitive to temperature and humidity due to various factors, 1) cold engine starts that enhance emissions at lower ambient temperatures due to the incomplete fuel combustion, 2) evaporative losses of volatile organic compounds (VOCs) due to expansion and contraction caused by ambient diurnal temperature variations, 3) enhanced running emissions at higher ambient temperatures, 4)
165 atmospheric moisture suppression of high combustion temperatures that lower nitrogen oxide emissions at higher humidity, and 5) indirect increased emissions from air conditioning at higher ambient temperatures (Choi et al., 2017; Iodice and Senatore, 2014; Lindhjem et al., 2004; Mellios. et al., 2019; USEPA, 2015). McDonald *et al.* (2018) found that NO_x emissions from NEI estimated from the U.S. EPA’s MOVES are



170 under-estimated, leading to a failure of prediction of high ozone days (8-hr max ozone > 70 ppb). (McDonald et al., 2018)

The dependency of mobile emissions on local meteorology can vary by vehicle types (light-duty, heavy-duty, truck and bus), fuel types (gasoline, diesel, hybrid, and electric), road types (interstate, freeway, local roads), processes (vehicle start-up, running exhaust, break-tire wear, hot soak, and extended idling), vehicle speed for onroad vehicles, hour of day for off-network vehicles, as well as by pollutants such as CO, NO_x, SO₂, 175 NH₃, VOC, Particulate Matter (PM). Figure 1 shows the dependency of MOVES emission factors of CO, NO_x, VOC, and PM_{2.5} from gasoline-fueled vehicles on ambient temperature from onroad and off-network, respectively. All pollutant emissions vary with the temperature, particularly under lower speed. The CO, VOC and NO_x emissions increase with the temperature while opposite relationship is suggested between PM_{2.5} emissions and temperature, implying the complexity of meteorology impacts on different pollutant 180 emissions. For off-network emissions from gasoline-fueled vehicles, CO, NO_x and PM_{2.5} show negative correlations with temperature, while the VOC exhibits nonlinear response to the temperature variation. The largest meteorology dependency occurs in daytime when emissions are the greatest across a day. Further detailed meteorology dependency of MOVES emission factors on local meteorology can be found in Choi *et al.*, 2017.

185 2.3 SMOKE-MOVES Integration Tool

In 2010, U.S. EPA introduced the process-based onroad mobile emissions model, MOVES, which is a state-of-the-science MySQL database-driven software for calculating bottom-up vehicular emissions from onroad and off-network. Off-network emission processes (e.g., parked engine-off, engine starts, and idling, and fuel vapor venting) in MOVES are hour-dependent due to vehicle activity assumptions built into the MOVES 190 model; the emission rate in a unit of grams/mile/hour depends on both hour of the day and temperature. Onroad emission processes (e.g., running exhaust, crankcase running exhaust, brake wear, tire wear, and onroad evaporative), on the other hand, do not depend on the hour but are expressed in grams/mile.

MOVES is approved for use in official state implementation plan (SIP) submissions to EPA and for conformity emissions inventory development outside of California. Furthermore, it can be used to estimate 195 onroad vehicle emissions for a variety of different purposes: to evaluate the national and local emissions trends, to compare different emission scenarios, to analyze the benefits from mobile source control strategies, and to provide inputs for air quality modeling. Although MOVES estimates of mobile emissions include the dependence on vehicle activities and simulated hourly meteorology, its computational requirements are prohibitive in real-time air quality forecasting applications. To overcome these issues, the SMOKE-MOVES 200 tool was developed by integrating MOVES emission factor (EF) outputs with the SMOKE modeling system (Baek, 2010), with the objectives of reducing processing time, and improving the accuracy of mobile emissions for air quality modeling. The tool allows hourly mobile emissions estimates based on vehicle activity inventories (i.e., miles traveled, population, and operating hours), MOVES EFs (a function of vehicle type, road type, and local meteorology), and simulated hourly ambient temperatures, and humidity. It first 205 estimates spatially and temporally averaged county-level hourly meteorological inputs (temperatures and humidity). It then prepares driver and post-processing scripts to set up and run MOVES to generate county-specific MOVES EF lookup tables (LUT), and to sort them by average vehicle speed, ambient temperatures, humidity, operating hours, day of week, and/or hour of the day. Finally, the tool runs SMOKE to estimate air quality model-ready emissions using the MOVES EF LUTs with hourly meteorological inputs.

210 Based on the latest 2017 National Emissions Inventory (NEI) Emissions Modeling Platform (EMP) (USEPA, 2022), the county-specific individual MOVES EF LUT file size can range from 60MB up to 150MB, and



processing so many MOVES EF LUT files from the targeted counties in our modeling domain (e.g., 12kmx12km grid over U.S. Continental) require significant computational resources, such as memory and storage spaces.

215 Development of CMAQ-MetEmis Coupler One of the future key advances for current CMAQ in NAQFC application is developing a unified forecast system (UFS) with dynamically coupled process-based emissions modeling to provide atmospheric chemicals feedbacks to climate and meteorology, and to boost the air quality forecast modeling applications in seasonal-to-sub seasonal predictions. While biogenic emissions, bi-directional NH₃ from fertilizer applications, and point-source plume rise are dynamically coupled in CMAQ

220 “*inline*” as a part of NAQFC, these known meteorology-induced emissions sectors have little or no accounting of meteorological impacts in current operational chemical and aerosol forecasts but are represented with static, no-weather-aware annual or monthly county total emissions and standard monthly/weekly/daily temporal allocation profiles to disaggregate them on finer time scales for the hourly air quality forecasts. It often results in poor forecasting performance due to the poor spatiotemporal

225 representations of precursor pollutants during high ozone and PM_{2.5} episodes (Tong et al., 2012). In this study, we developed the meteorologically-induced emissions coupler module (MetEmis) within the CMAQ modeling system to enhance the current NAQFC with the weather-aware emissions modeling capability without any additional computational burden to the system. Pouliot (2005) indicated that the main obstacle to implementing weather-aware emissions into air quality simulation is a significant computational

230 resource requirement, especially for air quality forecasting applications. To address these potential shortcomings (computational time and memory requirements), we first implemented a new feature in the SMOKE v4.8.1 modeling system to generate the temperature-specific pre-gridded hourly emissions called “MetEmis_TBL”, and then store them into the pseudo-layer structure for easy and fast access for later weather-aware emissions estimations (Figure 2). Each pseudo-layer holds the pre-gridded hourly emissions

235 based on pre-defined temperature bins (e.g., 5°C, 10°C, 15°C, and so on). There are two ways to process the “MetEmis_TBL” emissions input file to develop weather-aware emissions: (a) “SMOKE-MetEmis”, and (b) “CMAQ-MetEmis”. The “SMOKE-MetEmis” is an “*offline*” approach based on the updated SMOKE modeling system with the “MetEmis_TBL” that can dynamically estimate weather-aware gridded hourly emissions with the forecast meteorology prior to the CMAQ simulations

240 (Figure 2a). The updated *Mrggrid* utility tool from the SMOKE will first read and process the “MetEmis_TBL” emissions file with the forecast meteorology as a part of the emissions processing step prior to the CMAQ simulations. However, the “CMAQ-MetEmis” is a true “*inline*” approach based on the CMAQ version 5.3.1 with a new dynamic emission coupler module called “MetEmis” that can internally generate weather-aware emissions with “MetEmis_TBL” within the CMAQ simulations (Figure 2b). While both

245 approaches generate the same CMAQ ready gridded weather-aware hourly emissions, the “CMAQ-MetEmis” approach will not only require any offline emissions modeling using SMOKE, but also expedite its computational processing time with the CMAQ parallelized simulations.

3. Results

In order to evaluate the impact of the “*MetEmis*” approach, the CMAQ modeling system is performed for two different scenarios, “*MetEmis*” and “*Base*”, respectively for the winter (January) and winter (July)

250 seasons of 2019. First, we analyze the response of NO_x, VOC, NH₃, and PM_{2.5} emissions to the dynamic “*inline*” SMOKE-MetEmis approach. Then, the evaluation of the CMAQ-MetEmis air quality modeling system is performed by the comparison of the simulated ambient concentrations of NO₂, O₃, and PM_{2.5} with



255 the observations where the most of meteorology-induced emissions are impacted by the meteorology compared to the “offline” static approach (i.e, Base).

3.1 Computational Efficiency

260 While estimating meteorologically-induced onroad mobile emissions using local meteorology accurately provides the emissions to CTM, the current “offline” SMOKE-MOVES integration tool approach has faced many challenges, such as computational burdens, and the data portability and distributions due to the size of data files and computationally expensive I/O data processing. Accurately generating the onroad mobile emissions for the U.S. continental using MOVES onroad emission model requires a significant amount of computational resources as well as the processing time. It approximately takes 12 computing hours to generate one county MOVES EF LUT table per month using MOVES (Baek et al., 2010). Simulating over

265 3,100 counties in the U.S. continental (CONUS) for 12 calendar months (>37,400 MOVES simulations) will require a tremendous amount of computational resources and time. Thus, U.S. EPA has adopted the representative county approach to reduce the number of counties as well as the number of modeling months. Each representative county was classified according to its state, altitude (high or low), fuel region, the presence of inspection and maintenance programs, the mean light-duty age, and the fraction of ramps (CRC, 270 2019). A total of 296 representative counties for CONUS and 38 for Alaska, Hawaii, Puerto Rico, and the US Virgin Islands (USEPA, 2022). Each representative county holds two fuel months to represent all 12 calendar months. Based on the 2017 NEI EMP, the county-specific individual MOVES EF LUT file size can range from 60MB up to 150MB, and there are a total of 668 MOVES EF LUT input files which represent 3,100 counties in the U.S. for an entire modeling year (334 LUT files per fuel month).

275 To generate one day (25 hourly time steps) CMAQ-ready gridded hourly emissions, SMOKE needs to read and process 334 MOVES EF LUT as well as many other SMOKE-ancillary input files such as VMT activity, temporal profiles, chemical speciation profiles, spatial surrogates, and so on. The most computational resources are consumed in I/O (inputs and outputs) of huge amount of data files while it processes the complex datasets. Table 2 shows the estimated computational resources and time per each onrad mobile sector (e.g., RatePerDistance (RPV), RatePerVehicle (RPV), and RatePerHour (RPH)). Among the mobile sectors, RPD and RPV are the slowest sectors processed in the SMOKE modeling system.

280 Based on the latest 2017 NEI EMP, CMAQ-ready gridded daily emissions in our modeling domain (e.g., 12kmx12km grid over U.S. Continental) requires approximately 1.9 hours per day (RPD: 90 minutes, RPV: 18 minutes, and RPH: 1 minute) to generate the complete set of onroad mobile daily emissions including RPD, RPV and RPH modes. It may require over 638.5 hours (~29 days) of computational time to generate CONUS gridded hourly emissions for 365 days. While the CMAQ-MetEmis “inline” approach (Figure 2b) does not cause much computational processing time since the I/O of NetCDF/IOAPI binary format MetEmis_TBL input file in the CMAQ modeling system is instantaneous. There was less than 1 minute per day of CMAQ computational time with 96 CPUs parallel processing.

290 The SMOKE-MetEmis can generate a single MetEmis_TBL emissions input file that holds the 25 temperature-bins gridded hourly emissions for 334 representative counties for one fuel month from 0°F to 125°F temperature (25 bins with 5°F increment). Correction equations for humidity are applied to estimate grid-cell-hour adjustment factors for NO_x emissions by fuel type (USEPA, 1997). The size of MetEmis_TBL input file that can represent the 334 MOVES LUTs files per fuel month with 25 temperature bins is

295 approximately 16GB which is significantly smaller than the size for 334 MOVES LUTs files, ~ 62.8GB.



Approximately 6 hours are required to generate the MetEmis_TBL file once with SMOKE per fuel month, prior to the CMAQ-MetEmis simulations.

3.2 Weather-Aware Mobile Emissions

300 The huge computational burden of traditional “offline” SMOKE-MOVES approach prohibits its usage in
providing real-time estimates of mobile emissions which might be significantly driven by the weather
changes, resulted in considerable uncertainties in predicting emissions and air quality. The spatial monthly
total difference plots of VOC and NO_x between “Base” and “MetEmis” from Figure 3 clearly show that most
of the emission differences caused by local meteorology occur from major interstate roads and metropolitan
305 cities (e.g., New York, Detroit, Chicago, Los Angeles, Phoenix, and Atlanta), where onroad mobile emissions
contribute the most. Especially, the most differences in VOC were occurred over California region in July
2019, probably because the original temporal profiles assumed in “Base” are not suitable to represent the real
condition influenced by the weather. The January and July VOC emissions from the “Base” scenario were
higher by over 8% and 20% than the ones from the “MetEmis” scenarios, respectively, indicating that current
310 NAQFC-ready onroad mobile emissions (no-weather-aware) are significantly over-representing the VOC
emissions compared to the weather-aware VOC dynamically estimated by MetEmis.

Unlike the “Base” approach, the “MetEmis” approach estimates hourly emissions by multiplying the
estimated hourly vehicle mileage traveled (VMT) in the unit of miles/hour with inventory pollutant emission
rates (unit of grams/miles), which are a function of local meteorology (e.g., ambient temperature and
315 humidity). The “MetEmis” emissions can enhance their spatiotemporal representations of onroad mobile
sources. However, the hourly VMT activity data is estimated using the same temporal profiles used in the
“Base” hourly emissions. Thus, both onroad emissions follow similar weekly and daily patterns with some
hourly variations based on local meteorological conditions. As presented in Figure 4 which compares the
hourly domain total TOG (Total Organic Gases), NO_x, and PM_{2.5} emissions between the “Base” and the
320 “MetEmis” approach, the statically estimated “Base” hourly emissions (colored blue) clearly show the
repeated weekly patterns within the same month due to the usage of the static weekly temporal profiles, while
the “MetEmis” (colored in red) display irregular hourly patterns due to the impacts of local hourly
meteorology.

Due to the influence of local meteorology (i.e., ambient temperature and relative humidity), the onroad
325 running exhaust/evaporative emissions from RPD and the off-network evaporative emissions from RPV
modes shows a moderate decrease of TOG and a slight increase of NO_x (> 4% increase) over the entire
domain due to low ambient and humidity condition during the winter season (January), according to
“MetEmis” estimates. The most important enhancement in “MetEmis” approach is that it allows modelers to
simulate NAQFC-ready weather-aware onroad mobile emissions. More important, the daily differences are
330 also noticeable in “MetEmis” approach within one month, as higher TOG and PM_{2.5} are shown in late January
due to the increased temperature, while the “Base” approach failed to predict such variation. Such
spatiotemporal enhancements of onroad mobile emissions predicted by “MetEmis”, especially near
metropolitan regions, would benefit the NAQFC.

335 3.3 Effects of Weather-Aware Mobile Emissions on simulations

This study investigated the response of NO₂, O₃ and PM_{2.5} to the meteorology-induced mobile emission
changes by simulating air quality under two scenarios (Base and MetEmis). The sensitivity of air pollutant
concentrations to these meteorology-induced emission sources was performed and analyzed in this section.



340 The monthly statistical modeling evaluation metrics for these two simulations (Base and MetEmis) over the
CONUS domain are provided in Table 3. The correlation coefficient (CORR) of O₃ is 0.51 for both
simulations, and they have the same normalized mean bias and errors (NMB and NME), while the relative
mean square error (RMSE) of Base (7.03 ppb) is slightly higher than that of MetEmis (7 ppb). The
simulated NO₂ shows the best correlations (0.64) among these three pollutants in January, however, its
RMSE, NMB, and NME are the largest. The PM_{2.5} simulation didn't reproduce the variability very well
345 with a lower CORR of 0.46, but it presents the best RMSE and moderate NMB/NME. In July, the CORRs
of O₃ improve from 0.51 to 0.64, while the RMSEs are also increasing because of intense concentration in
summer. The NO₂ and PM_{2.5} have the opposite pattern compared to that of O₃ with decreased CORR (0.51
and 0.38, respectively) and improved biases and errors, except the NME of NO₂. Over the entire modeling
domain, both simulations show quite similar modeling performances against the observations, with the
350 difference generally below 1%. This is mostly attributable to the spatial pattern of emissions which is
primarily concentrated in urban areas. The most impacts of MetEmis emissions are shown over
metropolitan cities where mobile emissions play a critical role in their local air quality.
Figure 5 shows the monthly average NO₂, O₃, and PM_{2.5} concentrations from the Base scenario and the
monthly average difference between the Base and MetEmis scenarios in July 2019. The spatial distributions
355 of simulated NO₂ present a close pattern with those of NO_x emission in both two months, demonstrating the
effect of local NO_x emission on the NO₂ activities. The NO₂ concentration in July is lower than January,
which is caused by the stronger NO₂ photolysis and ventilation. In January, the NO₂ simulated by MetEmis
showed higher concentration over the domain with more than 0.2 ppb larger over urban areas because of
the increased NO_x emission after adjustment. In comparison, the monthly simulated NO₂ concentrations
360 with and without emission adjustment are much closer in July, the emission adjustment makes the
concentration increase in the east while a decrease in the west. Compared to NO₂, the secondary O₃ and
PM_{2.5} formation chemical reactions involve complex nonlinear processes under various meteorological
conditions and precursor emissions. Despite their complexity, there are strong correlations between their
nonlinear responses and precursor emission changes.
365 The O₃ concentration is generally below 36 ppb in most areas in January because of the cold weather and
weak photolysis process, while it presents high over the mid-western US which is caused by the higher
altitude over the Rocky Mountains area. The O₃ significantly increases in July with average concentration of
43.9 ppb, which is 10 ppb larger than that in January. In July, the northeastern US becomes the hot spot zone
as the local anthropogenic emission and pollution transport are both strong. In the meanwhile, the O₃ also
370 concentrated over the water, such as Great Lake and northeastern coastal areas. The most of ozone increase
occurred around the surrounding regions of metropolitan cities like Chicago, IL, Atlanta, GA, Denver, CO
and Phoenix, AZ, where both NO_x and VOC emissions are slightly increased during July 2019 (Figure 3).
However, San Jose area shows a significant decrease of ozone during the summer in 2019 due to the higher
VOC estimations from NEI (Base) compared to the ones from MetEmis scenario (Figure 3).
375 The PM_{2.5} simulation has similar patterns in January and July with more particles concentrating in the east.
The southwestern areas show less particulate pollution as the emission we use does not include natural
sources such as dust storms and wildfires. The results from MetEmis present slightly higher PM_{2.5} in the east
because of the increased primary PM_{2.5} emission. In addition, a decreased PM_{2.5} concentration is noted in
California. This may attribute to the less generated secondary aerosols as the VOC emission is significantly
380 reduced after adjustment.



3.4 Evaluation on Modeling Performance

This study further examines the influence of meteorology-induced mobile emission changes on modeling performance which is particularly important for the air quality forecasting in NAQFC. 10 cities with the most changes in emissions are selected for comparison, as shown in Figure 6. In general, noticeable
385 improvement is found in NO₂ simulation with increase R² in all 10 cities except Detroit. San Jose and Atlanta exhibits the largest improvement in NO₂ simulation. Apparently, the MetEmis successfully captured daily variations of mobile emissions, resulted in an improved temporal correlation. Meanwhile, the RMSEs were reduced in most of cities (8 out of 10), suggesting the simulated biases can also be eliminated with MetEmis.

390 Compared to NO₂, changes in O₃ and PM_{2.5} are smaller due to the complex reactions. However, improvement is also found in summer with increased R² and reduced RMSE in more than 70% cities, though less improvement is suggested in winter. We analyzed a few episodes with the largest changes for O₃ and PM_{2.5} to better demonstrate such improvement.

395 **Ozone Episodes Analysis**

Based on the July 2019 CMAQ simulation between the Base and MetEmis cases, we identified the locations where the largest changes in surface ozone occurred. Especially, in July 2019, we witnessed a significant decrease in ozone over San Jose, CA at 1:00 PM local time on July 24, 2019, while the most increase in ozone occurred over Chicago, IL at 11:00 AM on July 5, 2019 (Table 4). Thus, we investigated
400 these two episodes to understand what the main drivers of these behaviors are.

Largest Ozone Increase Episode

Figure 7 shows the spatial ozone concentrations and the differences over Chicago region between the Base and MetEmis scenarios at 11AM LST on July 5, 2019. While the highest ozone occurred around the south
405 of Michigan lake in both scenarios (Figure 7a), the largest ozone increase (~7ppb) is shown in the middle of Michigan lake, where unfortunately there is no AQS monitoring location (Figure 7b). To understand the cause of these ozone changes, we examined the differences of NO_x and VOC emissions between Base and MetEmis scenarios. The increase of VOC emissions from the MetEmis scenario in the early morning (3LST-9LST) over the VOC limited Chicago, IL region seems to be the main driver of a significant
410 increase of ozone (Figure 8). The detailed information on VOC and NO_x concentration changes on July 5th, 2019, is listed in Table 5. In the early morning, there was a decrease in NO_x concentration, and an increase in VOC concentrations over Chicago area. Due to no monitoring location available over the lake, we were not able to properly perform the modeling evaluation statistics during the largest ozone increase.

415 *Largest Ozone Decrease Episode*

There was more than an 80ppb ozone decrease over San Jose, CA at 11LST on July 24th, 2019. To understand the cause of this significant decrease, we performed the analysis of precursor emissions changes during the episode period. The colored green AQS locations are selected for the ozone concentration analysis, while the red ones are for the PM_{2.5} monitoring locations (Figure 9a). Figure 9b shows the
420 modeled hourly ozone concentrations (maximum, minimum, and mean) and AQS observations over the blue box targeted region from Figure 9a. Figure 9b and Figure 10 indicate that the maximum ozone values from “Base” scenario clearly show an overestimated ozone over San Jose, CA downwind region, while the MetEmis case shows a significant improvement in maximum ozone concentration during the daytime. The



425 main driver of this significant ozone change over the San Jose targeted area is due to the substantial
reduction in VOC emissions in MetEmis from Base (Figure 11a). Statistics of NO_x and VOC
concentrations from CMAQ in Table 6 show consistent findings.

Largest PM_{2.5} Decrease Episodes

430 Along with the significant ozone decrease in July, 2019, there was a significant PM_{2.5} decrease from
CMAQ-MetEmis simulation from 42.5 μg/m³ (Base) to 25 μg/m³ at 10LST on January 3, 2019.
Approximately 17.5 μg/m³ (>41%) PM_{2.5} decrease was witnessed in CMAQ-MetEmis simulations (Figure
11). The CMAQ-MetEmis simulation shows a significant improvement in modeled PM_{2.5} concentration,
compared to the one from the AQS monitoring locations from 8a (Figure 12a). The main cause of this
PM_{2.5} decrease in CMAQ-MetEmis is mainly a significant decrease in primary PM_{2.5} and VOC emissions
435 (Figure 13). Primary hourly PM_{2.5} emissions from MetEmis scenario were significantly lowered than the
ones from Base scenario, approximately a maximum of 20kg/hour from 3LST to 9LST on January 3, 2019.

4. Conclusions

To address the limitation of traditional estimation for onroad vehicle emissions, this study developed a novel
method (*i.e.*, MetEmis) by dynamically coupling the meteorology-induced onroad emissions with simulated
440 meteorological data in the air quality modeling system, which significantly improves both computational
efficiency and accuracy. The computational time for processing one day onroad emission data is substantially
reduced from 1.9 hours offline to less than 1 minute inline, enabling the onroad emission estimates
simultaneously coupled with the meteorology forecasting. Overall, the MetEmis corrected the low-biases of
NO_x and primary PM_{2.5} emissions domain wide, and high-biases of VOC emissions in California. The
445 MetEmis also successfully captured the temporal variation of onroad vehicle emissions, resulted in an
improved simulated NO₂, O₃ and PM_{2.5} concentrations with more agreement with observations compared to
the ones using static temporal profiles. Particularly, the simulated NO₂ concentration exhibits noticeable
improvement with increased R² and decreased RMSEs in most cities. The simulated O₃ and PM_{2.5}
concentrations were also improved, particularly in summer.

450 The newly developed CMAQ-MetEmis model demonstrates the importance of dynamic-coupling emissions
and meteorological forecasting. While this study only focused on the onroad emissions, other meteorology-
induced sectors such as residential combustions and agricultural livestock are planned to be included in the
MetEmis development to well represent the meteorological influence on all meteorologically-induced
anthropogenic emissions.

455



Digital Object Identifier (DOI) for the CMAQ-MetEmis Coupler:

<https://doi.org/10.5281/zenodo.7150000>

Code Availability:

460 The source codes of the SMOKE and the CMAQ models for MetEmis coupler can be downloaded from the DOI website (<https://doi.org/10.5281/zenodo.7150000>)

Data availability:

All the datasets, excel and python scripts used in this manuscript for the data analysis are uploaded through the DOI website (<https://doi.org/10.5281/zenodo.7150000>)

465 Author contribution

Dr. B.H. Baek is the lead researcher in this study, and Drs. Baek and Coats developed the source codes of CMAQ-MetEmis. Drs. Ma, Wang, Xing and Tong prepared the modeling inputs and analyzed the modeling results. Drs. Woo and Kim participated in the design of the weather-aware emission modeling system.

Competing interests

470 The Authors declare that they have no conflict of interest.

Acknowledgments

This research was funded by the National Oceanic and Atmospheric Administration (NOAA)'s Office of Weather and Air Quality (OWAQ) to improve the National Air Quality Forecasting Capability (NAQFC) (Award: NOAA-OAR-OWAQ-2019-2005820) and National Strategic Project-Fine Particle of the National
475 Research Foundation (NRF) of Korea funded by the Ministry of Science and ICT (MSIT), the Ministry of Environment (ME), the Ministry of Health and Welfare (MOHW) (NRF-2017M3D8A1092022), and by the Korea Environmental Industry & Technology Institute (KEITI) through the Public Technology Program based on Environmental Policy Program, funded by Korea Ministry of Environment (MOE) (2019000160007).

480 References

Andrade, M. d. F., Kumar, P., de Freitas, E. D., Ynoue, R. Y., Martins, J., Martins, L. D., Nogueira, T., Perez-Martinez, P., de Miranda, R. M., Albuquerque, T., Gonçalves, F. L. T., Oyama, B., and Zhang, Y.: Air quality in the megacity of São Paulo: Evolution over the last 30 years and future perspectives, *Atmospheric Environment*, 159, 66-82, <https://doi.org/10.1016/j.atmosenv.2017.03.051>, 2017.

485 Baek, B. H.: Integration approach of MOVES and SMOKE models, the 19th Emissions Inventory Conference, San Antonio, TX2010.

Baek, B. H. and Seppanen, C.: CEMPD/SMOKE: SMOKE v4.8.1 Public Release (January 29, 2021) (SMOKEv481_Jan2021): <https://doi.org/10.5281/zenodo.4480334>, last access: Nov 4th.

490 Baek, B. H., Seppanen, C., Houyoux, M., Eyth, A., and Mason, R.: Installation Guide for the SMOKE-MOVES Integration Tool, 2010.



- Byun, D. and Schere, K. L.: Review of the Governing Equations, Computational Algorithms, and Other Components of the Models-3 Community Multiscale Air Quality (CMAQ) Modeling System, *Applied Mechanics Reviews*, 59, 51-77, 10.1115/1.2128636, 2006.
- 495 Chen, D., Liang, D., Li, L., Guo, X., Lang, J., & Zhou, Y.: The temporal and spatial changes of ship-contributed PM_{2.5} due to the inter-annual meteorological variation in Yangtze river delta, China, *Atmosphere*, 12(6), 722, 2021.
- 500 Chen, W. H., Guenther, A. B., Wang, X. M., Chen, Y. H., Gu, D. S., Chang, M., Zhou, S. Z., Wu, L. L., and Zhang, Y. Q.: Regional to Global Biogenic Isoprene Emission Responses to Changes in Vegetation From 2000 to 2015, *Journal of Geophysical Research: Atmospheres*, 123, 3757-3771, 10.1002/2017jd027934, 2018.
- Choi, D., Beardsley, M., Brzezinski, D., Koupal, J., and Warila, J.: MOVES Sensitivity Analysis: The Impacts of Temperature and Humidity on Emissions, 2017.
- 505 Dennis, R., Fox, T., Fuentes, M., Gilliland, A., Hanna, S., Hogrefe, C., Irwin, J., Rao, S. T., Scheffe, R., Schere, K., Steyn, D., and Venkatram, A.: A FRAMEWORK FOR EVALUATING REGIONAL-SCALE NUMERICAL PHOTOCHEMICAL MODELING SYSTEMS, *Environ Fluid Mech (Dordr)*, 10, 471-489, 10.1007/s10652-009-9163-2, 2010.
- 510 Esri, D., HERE, TomTom, Intermap, increment P Corp., GEBCO, USGS, FAO, NPS, NRCAN, GeoBase, IGN, Kadaster NL, Ordnance Survey, Esri Japan, METI, Esri China (Hong Kong), Swisstopo, MapmyIndia, and the GIS User Community: World Topographic Map, 2013.
- 515 Fiore, A. M., Naik, V., Spracklen, D. V., Steiner, A., Unger, N., Prather, M., Bergmann, D., Cameron-Smith, P. J., Cionni, I., Collins, W. J., Dalsøren, S., Eyring, V., Folberth, G. A., Ginoux, P., Horowitz, L. W., Josse, B., Lamarque, J. F., MacKenzie, I. A., Nagashima, T., O'Connor, F. M., Righi, M., Rumbold, S. T., Shindell, D. T., Skeie, R. B., Sudo, K., Szopa, S., Takemura, T., and Zeng, G.: Global air quality and climate, *Chem Soc Rev*, 41, 6663-6683, 10.1039/c2cs35095e, 2012.
- Foltescu, V. L., Pryor, S. C., and Bennet, C.: Sea salt generation, dispersion and removal on the regional scale, *Atmospheric Environment*, 39, 2123-2133, <https://doi.org/10.1016/j.atmosenv.2004.12.030>, 2005.
- 520 Grell, G. and Baklanov, A.: Integrated modeling for forecasting weather and air quality: A call for fully coupled approaches, *Atmospheric Environment*, 45, 6845-6851, <https://doi.org/10.1016/j.atmosenv.2011.01.017>, 2011.
- Grell, G., Freitas, S. R., Stuefer, M., and Fast, J.: Inclusion of biomass burning in WRF-Chem: impact of wildfires on weather forecasts, *Atmos. Chem. Phys.*, 11, 5289-5303, 10.5194/acp-11-5289-2011, 2011.
- Hogrefe, C., Rao, S. T., Kasibhatla, P., Kallos, G., Tremback, C. J., Hao, W., Olerud, D., Xiu, A., McHenry, J., and Alapaty, K.: Evaluating the performance of regional-scale photochemical modeling systems: Part I—



- 525 meteorological predictions, *Atmospheric Environment*, 35, 4159-4174, [https://doi.org/10.1016/S1352-2310\(01\)00182-0](https://doi.org/10.1016/S1352-2310(01)00182-0), 2001.
- Iodice, P. and Senatore, A.: Cold Start Emissions of a Motorcycle Using Ethanol-gasoline Blended Fuels, *Energy Procedia*, 45, 809-818, <https://doi.org/10.1016/j.egypro.2014.01.086>, 2014.
- Jacob, D. J. and Winner, D. A.: Effect of climate change on air quality, *Atmospheric Environment*, 43, 51-63, <https://doi.org/10.1016/j.atmosenv.2008.09.051>, 2009.
- 530 Knippertz, P. and Todd, M. C.: Mineral dust aerosols over the Sahara: Meteorological controls on emission and transport and implications for modeling, *Reviews of Geophysics*, 50, 10.1029/2011rg000362, 2012.
- Kumar, P., Patton, A. P., Durant, J. L., and Frey, H. C.: A review of factors impacting exposure to PM_{2.5}, ultrafine particles and black carbon in Asian transport microenvironments, *Atmospheric Environment*, 187, 301-316, <https://doi.org/10.1016/j.atmosenv.2018.05.046>, 2018.
- 535 Lathière, J., Hauglustaine, D. A., De Noblet-Ducoudré, N., Krinner, G., and Folberth, G. A.: Past and future changes in biogenic volatile organic compound emissions simulated with a global dynamic vegetation model, *Geophysical Research Letters*, 32, <https://doi.org/10.1029/2005GL024164>, 2005.
- Lee, P., McQueen, J., Stajner, I., Huang, J., Pan, L., Tong, D., Kim, H., Tang, Y., Kondragunta, S., Ruminski, M., Lu, S., Rogers, E., Saylor, R., Shafran, P., Huang, H.-C., Gorline, J., Upadhayay, S., and Artz, R.: NAQFC Developmental Forecast Guidance for Fine Particulate Matter (PM_{2.5}), *Weather and Forecasting*, 32, 343-360, 10.1175/waf-d-15-0163.1, 2017.
- 540 Li, Q., Qiao, F., and yu, L.: Vehicle Emission Implications of Drivers Smart Advisory System for Traffic Operations in Work Zones, *Journal of the Air & Waste Management Association*, 11, 10.1080/10962247.2016.1140095, 2016.
- 545 Lindhjem, C., Chan, L., Pollack, A., Corporation, E. I., Way, R., and Kite, C.: Applying Humidity and Temperature Corrections to On and Off-Road Mobile Source Emissions, 13th International Emission Inventory Conference, Clearwater, FL2004.
- Liu, H., Guensler, R., Lu, H., Xu, Y., Xu, X., and Rodgers, M.: MOVES-Matrix for High-Performance On-Road Energy and Running Emission Rate Modeling Applications, *Journal of the Air & Waste Management Association*, 69, 10.1080/10962247.2019.1640806, 2019.
- 550 Luecken, D. J., Yarwood, G., and Hutzell, W. T.: Multipollutant modeling of ozone, reactive nitrogen and HAPs across the continental US with CMAQ-CB6, *Atmospheric Environment*, 201, 62-72, <https://doi.org/10.1016/j.atmosenv.2018.11.060>, 2019.



- 555 Lv, Z., Liu, H., Ying, Q., Fu, M., Meng, Z., Wang, Y., ... & He, K.: Impacts of shipping emissions on PM 2.5 pollution in China, *Atmospheric Chemistry and Physics*, 18(21), 15811-15824, 2018.
- McDonald, B. C., McKeen, S. A., Cui, Y. Y., Ahmadov, R., Kim, S. W., Frost, G. J., Pollack, I. B., Peischl, J., Ryerson, T. B., Holloway, J. S., Graus, M., Warneke, C., Gilman, J. B., de Gouw, J. A., Kaiser, J., Keutsch, F. N., Hanisco, T. F., Wolfe, G. M., and Trainer, M.: Modeling Ozone in the Eastern U.S. using a Fuel-Based Mobile Source Emissions Inventory, *Environ Sci Technol*, 52, 7360-7370, 10.1021/acs.est.8b00778, 2018.
- 560 Mellios., G., Ntziachristos, L., Samaras, Z., White, L., Martini, G., and Rose, K.: EMEP/EEA air pollutant emission inventory guidebook 2019, Gasoline evaporation, European Environment Agency 2019.
- Pavlovic, R., Chen, J., Anderson, K., Moran, M. D., Beaulieu, P. A., Davignon, D., and Cousineau, S.: The FireWork air quality forecast system with near-real-time biomass burning emissions: Recent developments and evaluation of performance for the 2015 North American wildfire season, *J Air Waste Manag Assoc*, 66, 819-841, 10.1080/10962247.2016.1158214, 2016.
- Perugu, H.: Emission modelling of light-duty vehicles in India using the revamped VSP-based MOVES model: The case study of Hyderabad, *Transportation Research Part D: Transport and Environment*, 68, 150-163, <https://doi.org/10.1016/j.trd.2018.01.031>, 2019.
- 570 Pierce, J. R. and Adams, P. J.: Global evaluation of CCN formation by direct emission of sea salt and growth of ultrafine sea salt, *Journal of Geophysical Research: Atmospheres*, 111, <https://doi.org/10.1029/2005JD006186>, 2006.
- Pouliot, G. A.: Emission processing for ETA/CMAQ, an air quality forecasting model, 7th Conference on Atmospheric Chemistry American Meteorological Society, San Diego, CA, January 09 - 13, 20052005.
- 575 Rao, S. T., Galmarini, S., and Puckett, K.: Air Quality Model Evaluation International Initiative (AQMEII): Advancing the State of the Science in Regional Photochemical Modeling and Its Applications, *Bulletin of the American Meteorological Society*, 92, 23-30, 10.1175/2010BAMS3069.1, 2011.
- Tang, Y., Pagowski, M., Chai, T., Pan, L., Lee, P., Baker, B., Kumar, R., Delle Monache, L., Tong, D., and Kim, H. C.: A case study of aerosol data assimilation with the Community Multi-scale Air Quality Model over the contiguous United States using 3D-Var and optimal interpolation methods, *Geosci. Model Dev.*, 10, 4743-4758, 10.5194/gmd-10-4743-2017, 2017.
- 580 Tong, D., Lee, P., and Saylor, R.: New Direction: The need to develop process-based emission forecasting models, *Atmospheric Environment*, 47, 560-561, 10.1016/j.atmosenv.2011.10.070, 2012.
- 585 Tong, D., Lamsal, L., Pan, L., Ding, C., Kim, H., Lee, P., Chai, T., Pickering, K. E., and Stajner, I.: Long-term NO_x trends over large cities in the United States during the great recession: Comparison of satellite



retrievals, ground observations, and emission inventories, *Atmospheric Environment*, 107, 70-84, <https://doi.org/10.1016/j.atmosenv.2015.01.035>, 2015.

590 Tong, D. & Mauzerall, D.L.: Spatial variability of summertime tropospheric ozone over the continental United States: Implications of an evaluation of the CMAQ model, *Atmospheric Environment*, 40(17), 3041-3056, 2006.

USEPA: Derivation of humidity and NOx humidity correction factors, 1997.

USEPA: Emission Adjustments for Temperature, Humidity, Air Conditioning, and Inspection and Maintenance for on-Road Vehicles in MOVES2014, 2015.

595 USEPA: MOVES and Other Mobile Source Emissions MOdel: <https://www.epa.gov/moves>, last

USEPA: 2017 Emissions Modeling Platform (EMP): <https://www.epa.gov/air-emissions-modeling/2017-emissions-modeling-platform>, last access: Nov 03.

600 Wong, K. W., Tsai, C., Lefer, B., Haman, C., Grossberg, N., Brune, W. H., Ren, X., Luke, W., and Stutz, J.: Daytime HONO vertical gradients during SHARP 2009 in Houston, TX, *Atmospheric Chemistry and Physics*, 12, 635-652, 10.5194/acp-12-635-2012, 2012.

Xu, X., Liu, H., Anderson, J. M., Xu, Y., Hunter, M. P., Rodgers, M. O., and Guensler, R. L.: Estimating Project-Level Vehicle Emissions with Vissim and MOVES-Matrix, *Transportation Research Record*, 2570, 107-117, 10.3141/2570-12, 2016.

605



Tables

Table 1. CMAQ modeling domain and configurations.

	<i>Base</i>	<i>MetEmis</i>
Horizontal Resolution	12km x 12km	
Meteorology	WRFv4.0 with GFS acting as ICs/BCs, RRTMG short/long wave scheme, Noah-MP land-surface scheme, YSU boundary layer scheme	
Boundary Condition	GEOS monthly product	
Initial Condition	CMAQ restart file	
Chemistry	CMAQv5.3.2 CB6r3 AE7	
Emissions	2017 NEI: Onroad monthly emissions	2017 NEI: Onroad Meteorology-induced emissions

610

Table 2. The required computational memory and time in the SMOKE modeling system.

Sector	Individual File Size	Total File Size (668 counties)	CPU Memory Usage (GB)	CPU Computing Time*
RPD	50-160 MB	62.8 GB	10~20	~ 90 mins/day
RPV	26-89 MB	34.5 GB	5~10	~ 18 mins/day
RPH	7-94 KB	43.6 MB	1~2	~ 1 mins/day

* The specification of CPU is Intel Xeon Gold 6240R @ 2.4GHz

615

Table 3. Statistical metrics between observed and simulated O₃, NO₂ and PM_{2.5} in January and July, 2019 over contiguous United States

	January 2019						July 2019					
	O ₃		NO ₂		PM _{2.5}		O ₃		NO ₂		PM _{2.5}	
	Base	MetEmis	Base	MetEmis	Base	MetEmis	Base	MetEmis	Base	MetEmis	Base	MetEmis
CORR	0.51	0.51	0.64	0.64	0.46	0.46	0.64	0.64	0.51	0.51	0.38	0.38
RMSE	7.03	7.00	8.33	8.27	5.72	5.76	9.56	9.51	5.69	5.67	5.03	5.04
NMB	-0.01	-0.01	-0.32	-0.30	0.10	0.11	-0.01	-0.01	-0.15	-0.15	-0.05	-0.05
NME	17%	17%	52%	52%	46%	47%	17%	17%	62%	62%	40%	40%

620



625

Table 4. The largest differences of ozone episodes in July 2019 over the U.S.

Episodes	Date @ Time	Base (ppb)	MetEmis (ppb)	Location
Largest Increase	Jul 5, 2019 @ 1PM	78.3	85.9 (+7.1)	Chicago, IL
Largest Decrease	Jul 24, 2019 @ 11AM	112.9	31.0 (-81.9)	San Jose, CA

630

Table 5. Summary of precursor (NO_x and VOC) concentrations in the morning before the largest ozone increase episode at 14LST on July 5th, 2019 over Chicago, IL.

Jul 5 th , 2019	NO _x (ppb)				VOC (ppbC)			
	Time	Base	MetEmis	Diff (M-B)	Time	Base	MetEmis	Diff (M-B)
Mean	5-11AM	8.4	8.6	0.2	5-11AM	62	66	4.0
Max	6-7AM	18.9	20.7	1.8	6-7AM	101	121	20.0
Min	6-7AM	8.5	8.2	-0.3	10-11AM	74	73	-1.0

635

Table 6. Statistics of largest ozone decrease episode (July 24th, 2019) over San Jose, CA.

Jul 24 th , 2019	NO _x (ppb)				VOC (ppbC)			
	Time	Base	MetEmis	Diff (M-B)	Time	Base	MetEmis	Diff (M-B)
Mean	3-9AM	5.8	6.8	1.0	3-9AM	184	35	148
Max	10-11AM	9.0	22.0	13.0	8-9AM	1263	68	-1195
Min	11-12pM	10.8	10.6	-0.2	12PM-1AM	7.8	7.3	-0.5



Figures

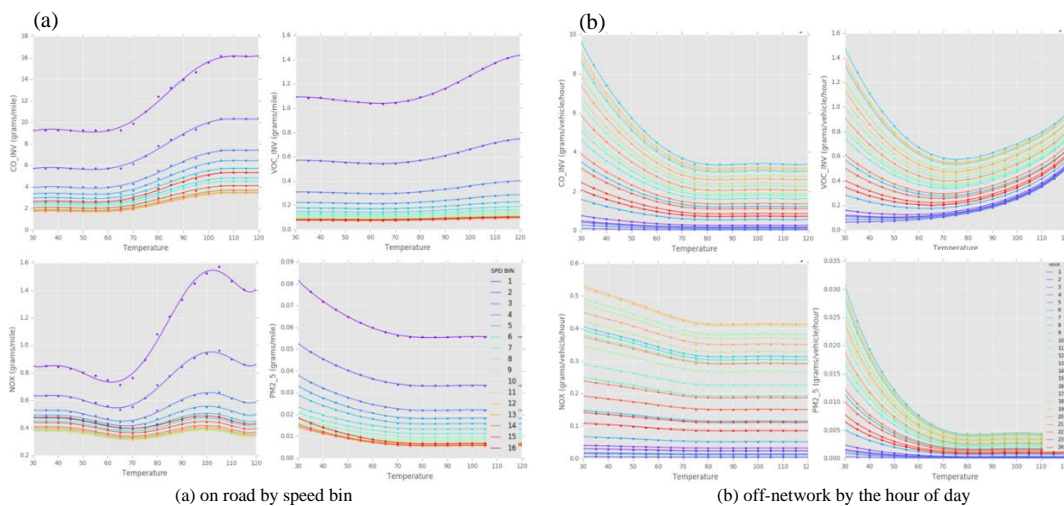


Figure 1. Meteorology-dependency of CO, VOC, NOx, and PM_{2.5} emissions from gasoline-fueled light-duty vehicles by average speed bin (a), and the off-network by the hour of day (b).

645

650

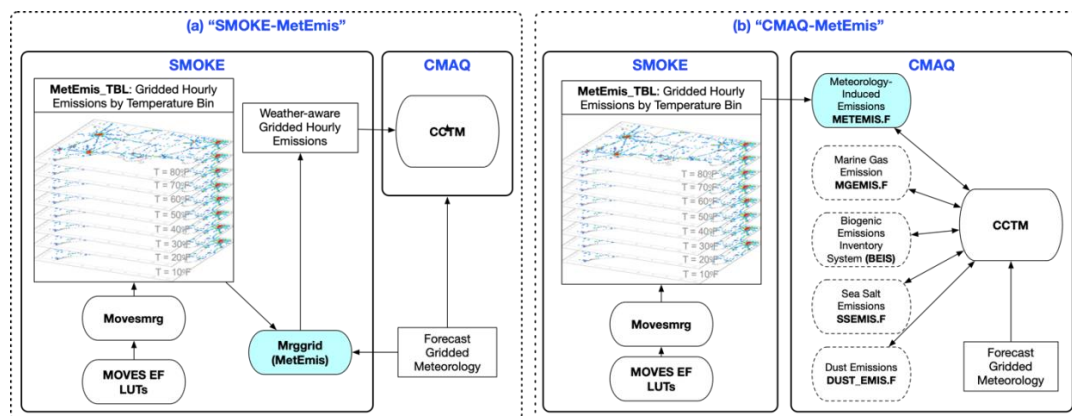


Figure 2. Meteorological-Induced Emissions coupler module "MetEmis" with air quality modeling system: a) "SMOKE-MetEmis", and b) "CMAQ-MetEmis".

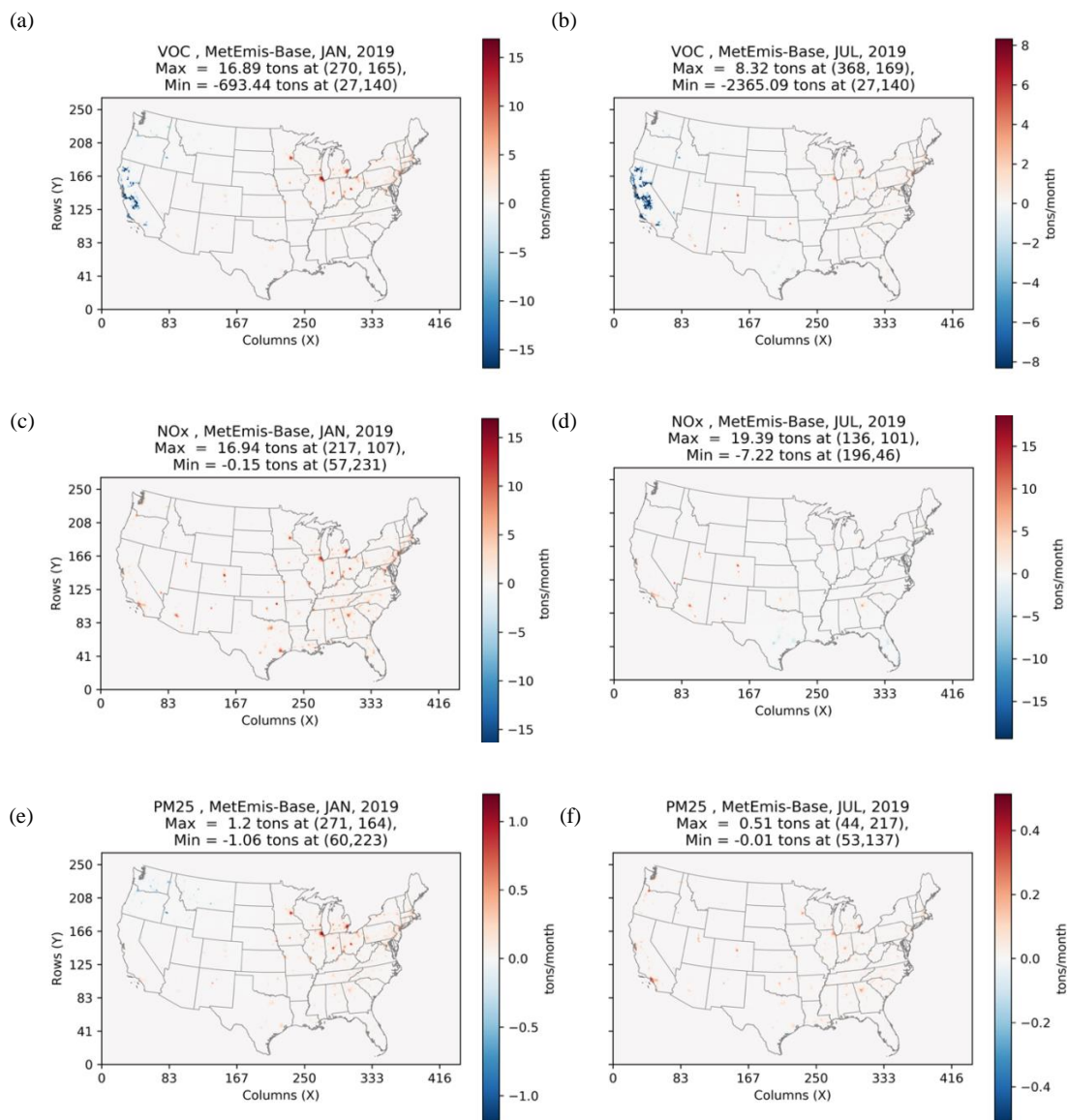


Figure 3. Spatial comparison of monthly total emissions of VOC, NO, and PM_{2.5}. The colors indicate the MetEmis is larger than Base (red) or smaller (blue) for (a) VOC in January, (b) VOC in July, (c) NO_x in January, (d) NO_x in July, (e) PM_{2.5} in January and (f) PM_{2.5} in July.

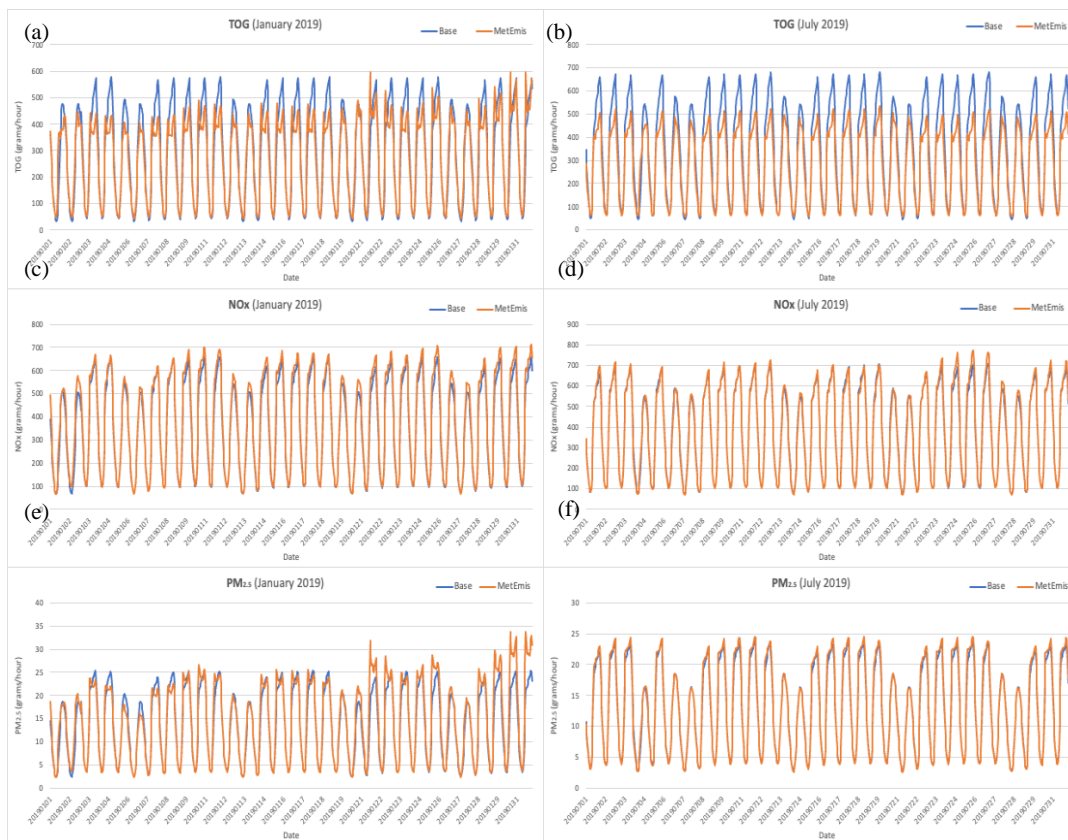
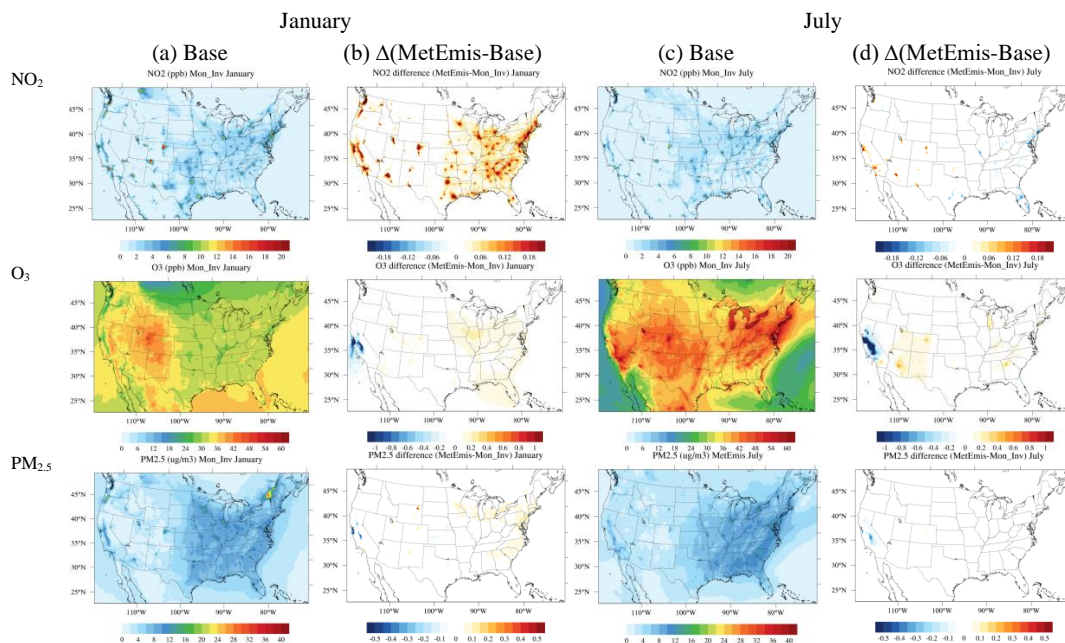


Figure 4. Temporal comparisons of daily domain total emissions of (a) Total Organic Gas (TOG) in January, (b) TOG in July, (c) NO_x in January, (d) NO_x in July, (e) PM_{2.5} in January and (f) PM_{2.5} in July from the Base (blue line) and MetEmis scenarios (red line).

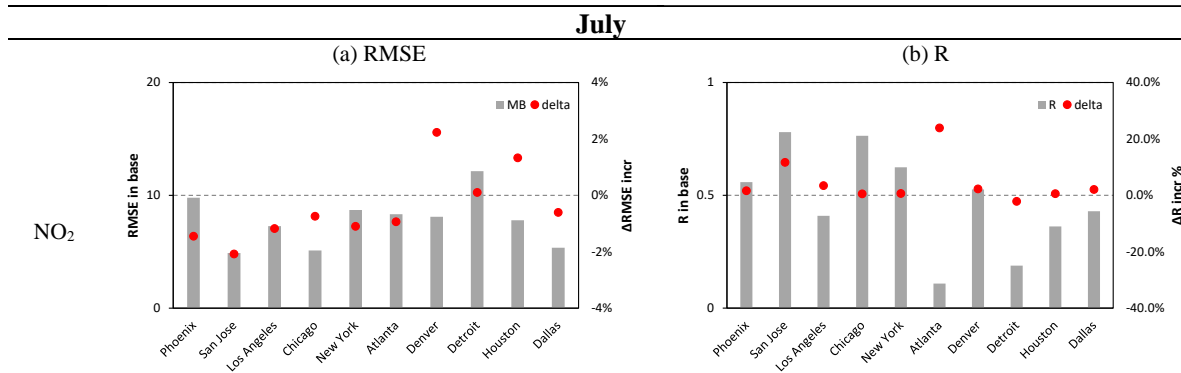
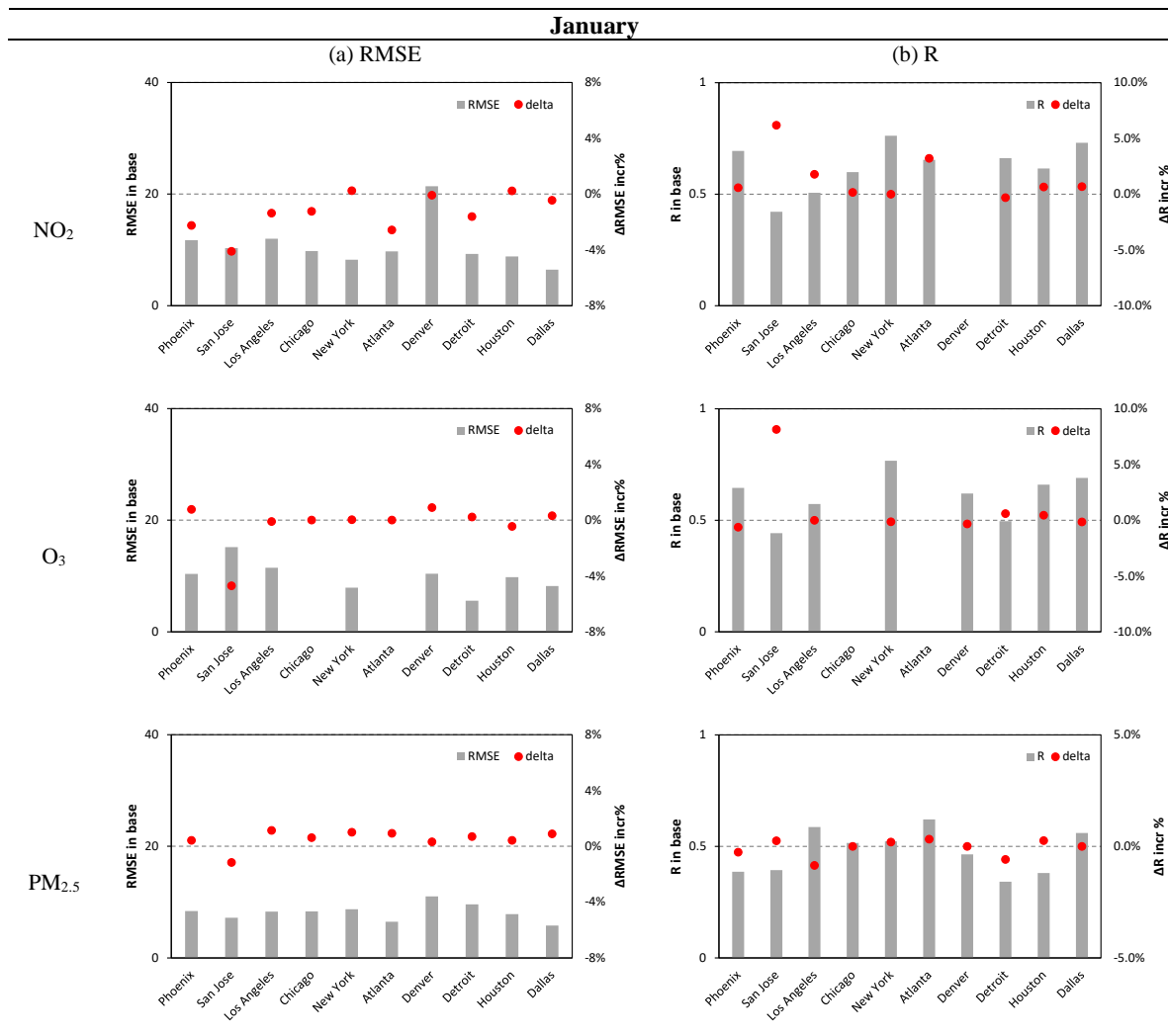


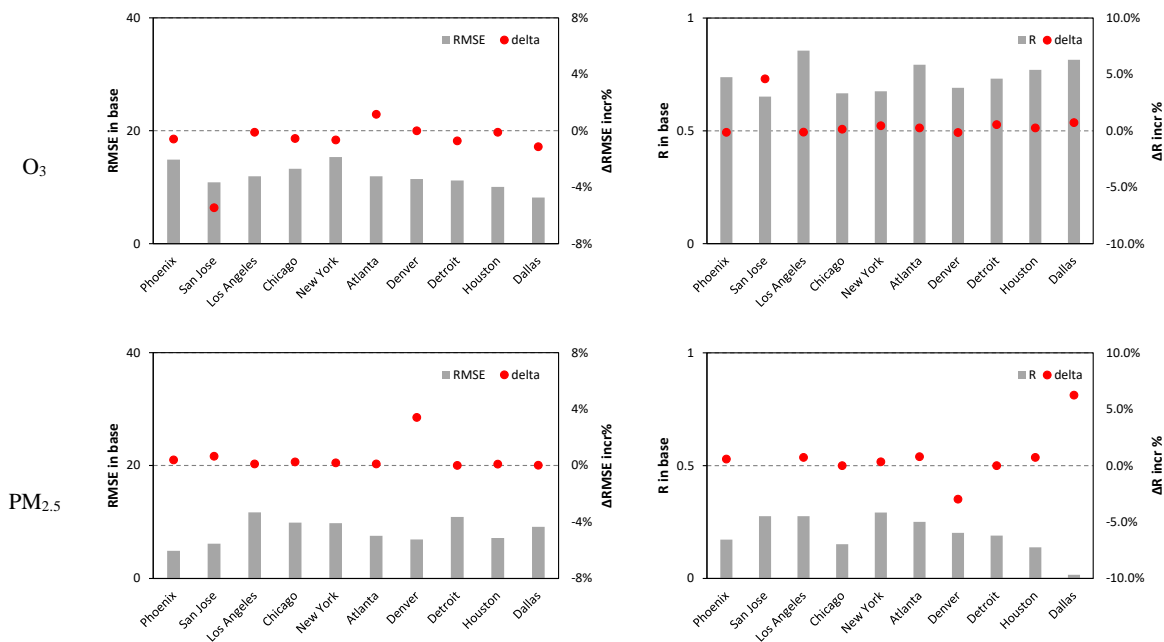
665



670

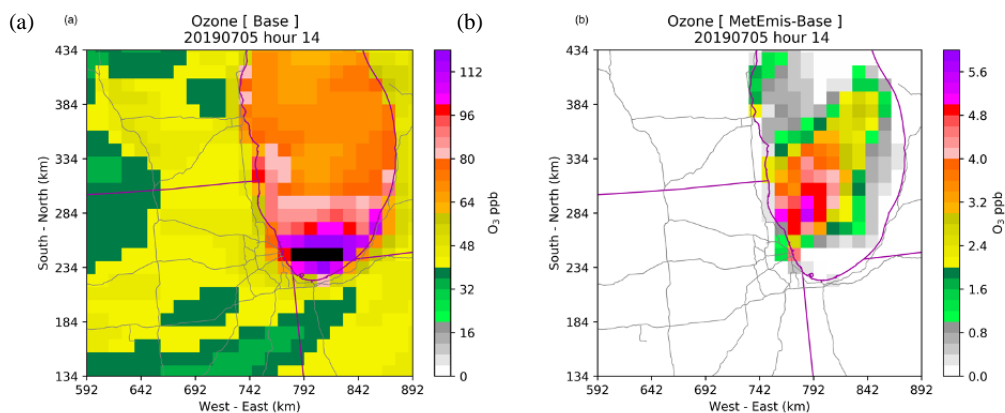
Figure 5. spatial distribution of NO_2 , O_3 and $\text{PM}_{2.5}$ concentrations and difference figures: (a) January averaged concentrations from Base scenario, (b) the differences between Base and MetEmiss scenarios in January, (c) July averaged concentrations from Base scenario, and (d) the differences between Base and MetEmiss scenarios in July





675 Figure 6. Comparison of model performance in simulating NO₂, O₃ and PM_{2.5} concentrations between Base and MetEmis scenarios. The columns panels shows the different model evaluation metrics in January (panel a and b) and July (panel c and d). The rows present different species including NO₂, O₃, and PM_{2.5}. RMSE is Root-mean-square deviation, R is correlation coefficient. delta is (MetEmis - Base)/Base; when ΔR > 0 and ΔRMSE < 0, indicate the improvement in MetEmis.

680 * NO₂ in January in Denver is -0.002, increased to 0.008 with MetEmis; Observed O₃ data is missing in Chicago and Atlanta in January.



685

Figure 7. Base hourly ozone (ppb) (a) and the hourly ozone difference (MetEmis-Base) (b) at 14LST on July 5th, 2019. Black color indicates the concentration above the color scale maximum (120 ppb)

690

695

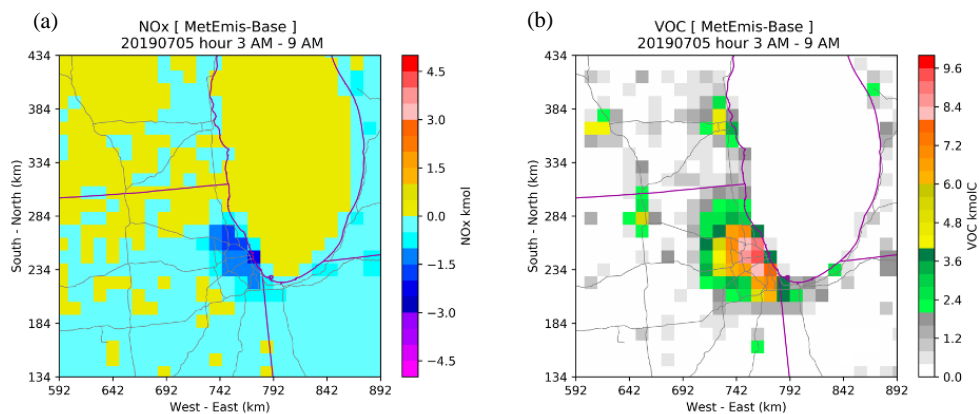


Figure 8. Spatial differences of NO_x (a) and VOC (b) emissions in early morning (3AM-9AM) on Jul 5th, 2019.

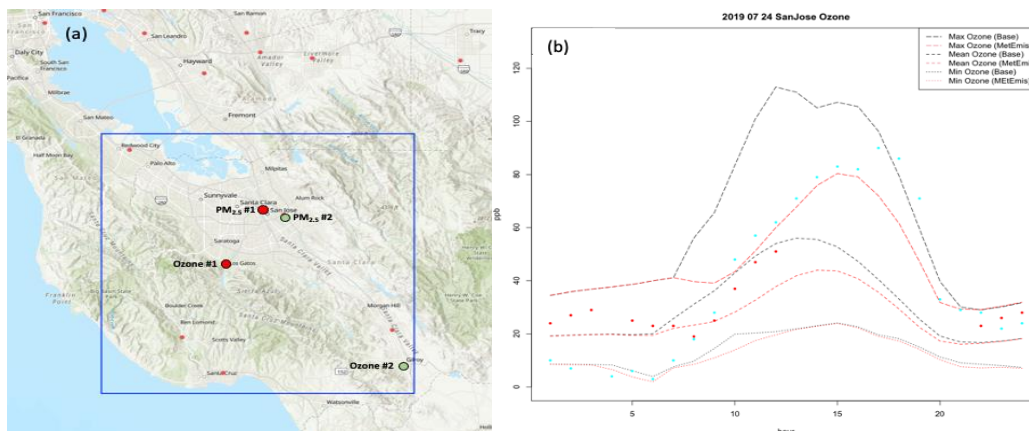


Figure 9. (a) U.S. EPA's Air Quality System (AQS) ozone and PM_{2.5} monitoring locations, and (b) diurnal variation of ozone (maximum, mean and minimum) on July 24, 2022 over San Jose, CA. The base map layer of this figure was made by Esri (Esri, 2013)

700

705

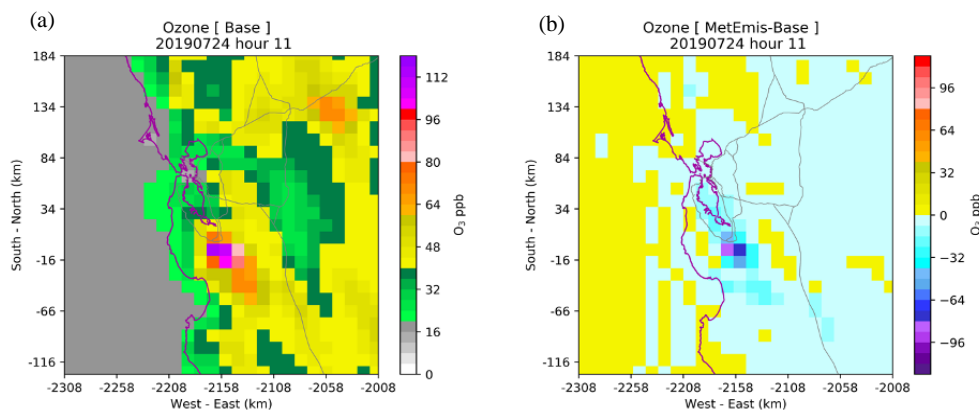


Figure 10. Base hourly ozone concentration (ppb) (a) and the hourly ozone difference (MetEms-Base) (b) at 11LST on July 24th, 2019.

710

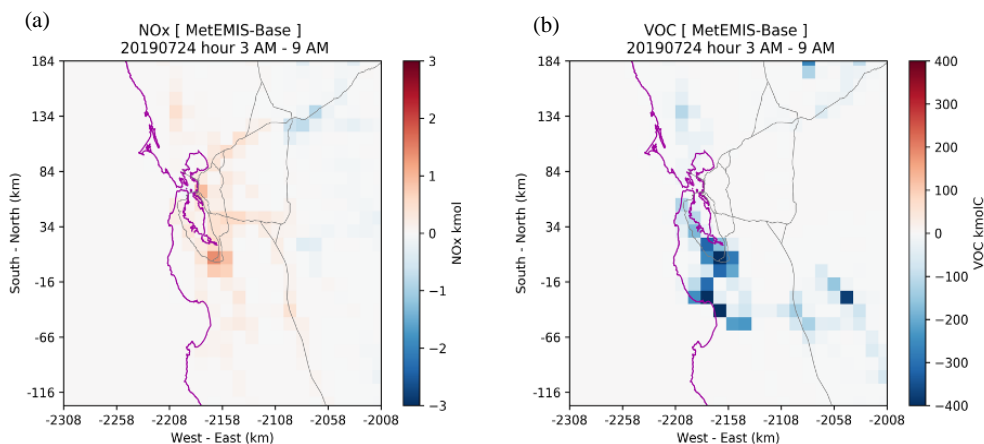


Figure 11. Spatial differences of NO_x (a) and VOC (b) emissions from 3LST to 9LST on July 24, 2019 over San Jose, CA.

715

720

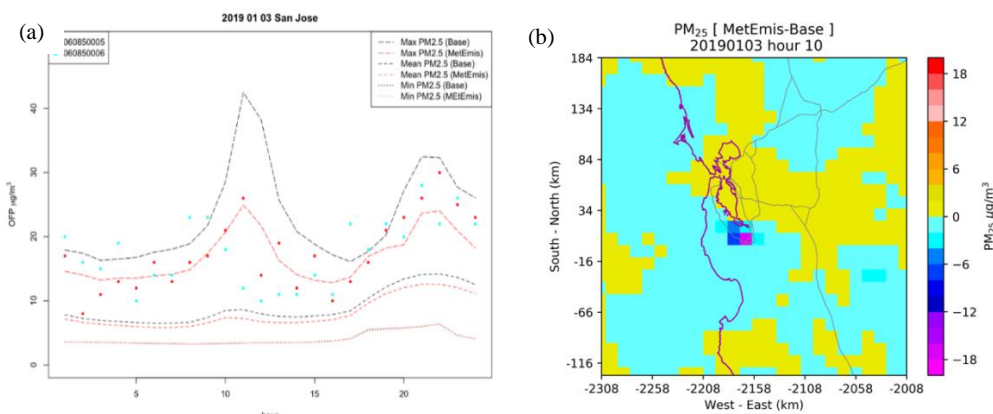


Figure 12. (a) Diurnal variation of PM_{2.5} (maximum, mean and minimum) concentrations over San Jose targeted region, and (b) the spatial difference of PM_{2.5} at 10LST on January 3, 2019.

725



730

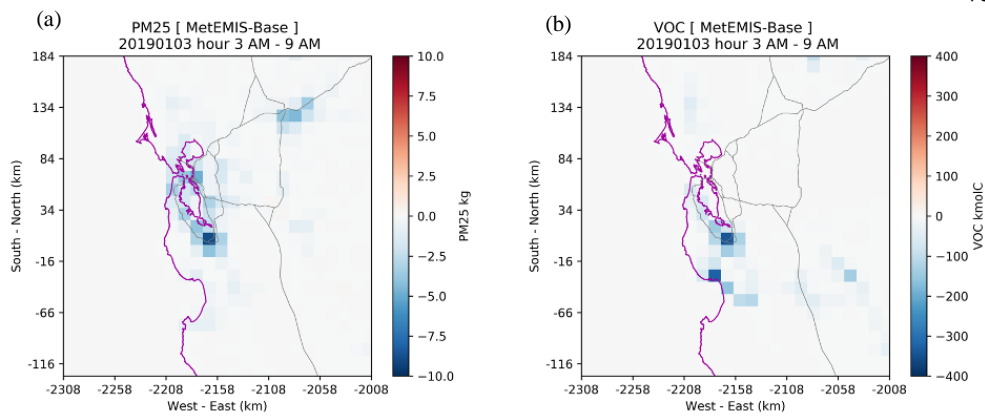


Figure 13. Spatial difference of PM_{2.5} (a) and VOC (b) emissions over San Jose region from 3LST to 9LST on January 3, 2019.